Electronic Supplementary Material (ESI) for Journal of Materials Chemistry A.

Double-atom catalysts: Transition metal dimer anchored C_2N monolayers as N_2 fixation electrocatalysts

Xu Zhang, An Chen, Zihe Zhang, Zhen Zhou*

School of Materials Science and Engineering, Institute of New Energy Material Chemistry, Computational Centre for Molecular Science, Nankai University, Tianjin 300350, P. R. China

*zhouzhen@nankai.edu.cn (Z.Z.).

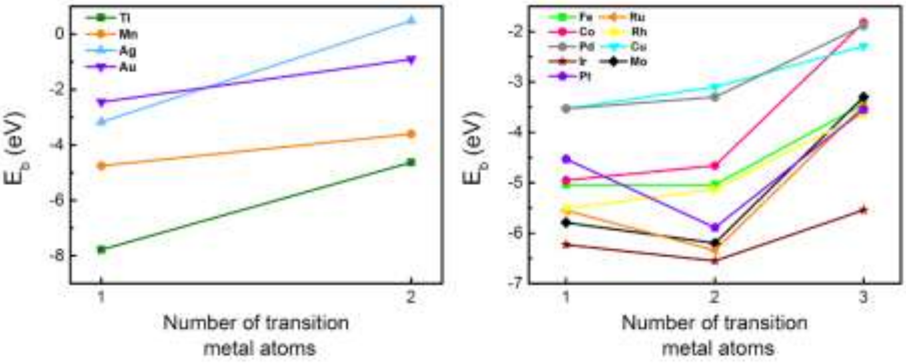

Fig. S1 Binding energies against the number of transition metal atoms.

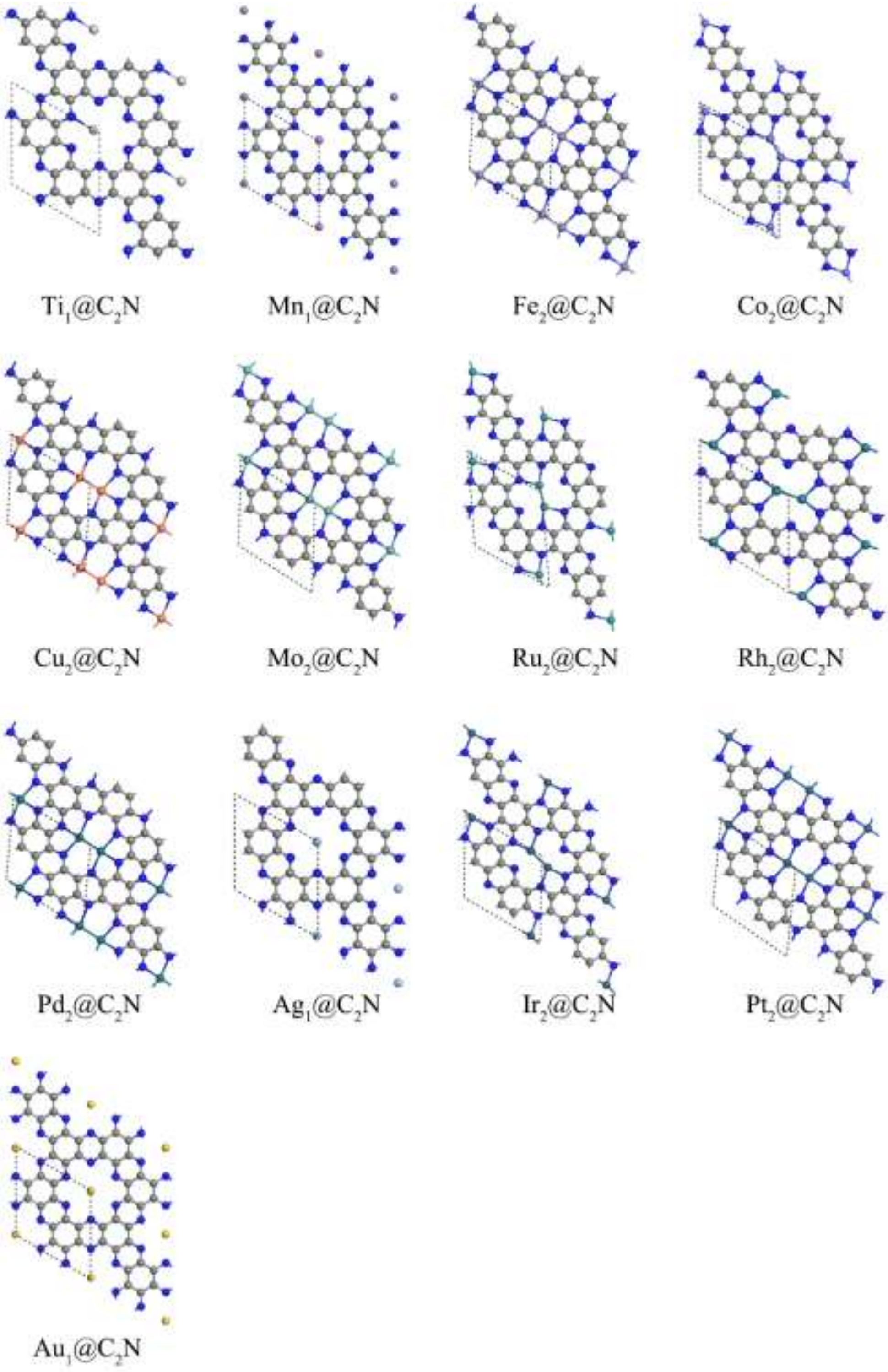

$Ti_1@C_2N$ $Mn_1@C_2N$ $Fe_2@C_2N$ $Co_2@C_2N$

$Cu_2@C_2N$ $Mo_2@C_2N$ $Ru_2@C_2N$ $Rh_2@C_2N$

$Pd_2@C_2N$ $Ag_1@C_2N$ $Ir_2@C_2N$ $Pt_2@C_2N$

$Au_1@C_2N$

Fig. S2 Optimized structures of the most stable $TM_x@C_2N$ catalysts. The blue and grey balls represent the nitrogen and carbon atoms, respectively. The areas circulated by dashed lines represent the unit cell.

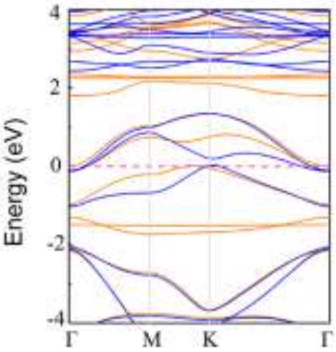

$Ti_1@C_2N$

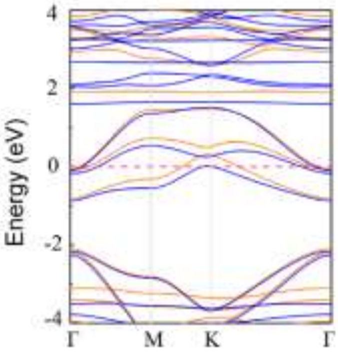

$Mn_1@C_2N$

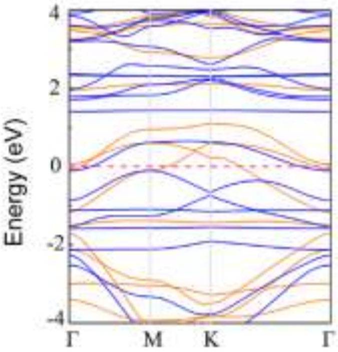

$Fe_1@C_2N$

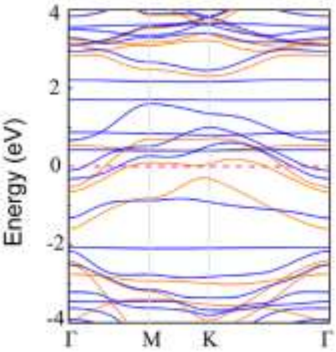

$Co_1@C_2N$

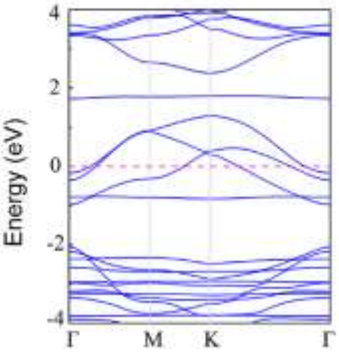

$Cu_1@C_2N$

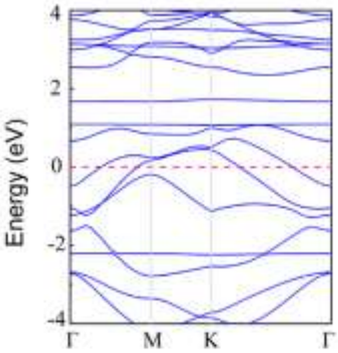

$Mo_2@C_2N$

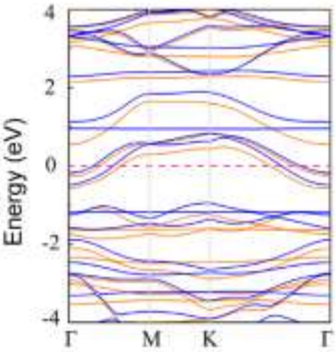

$Ru_2@C_2N$

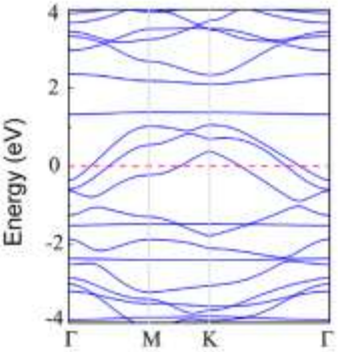

$Rh_2@C_2N$

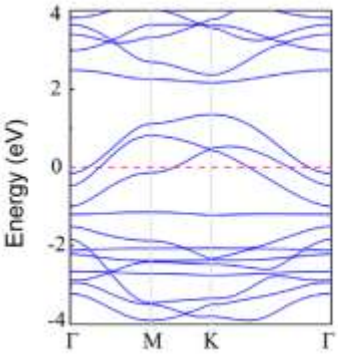

$Pd_2@C_2N$

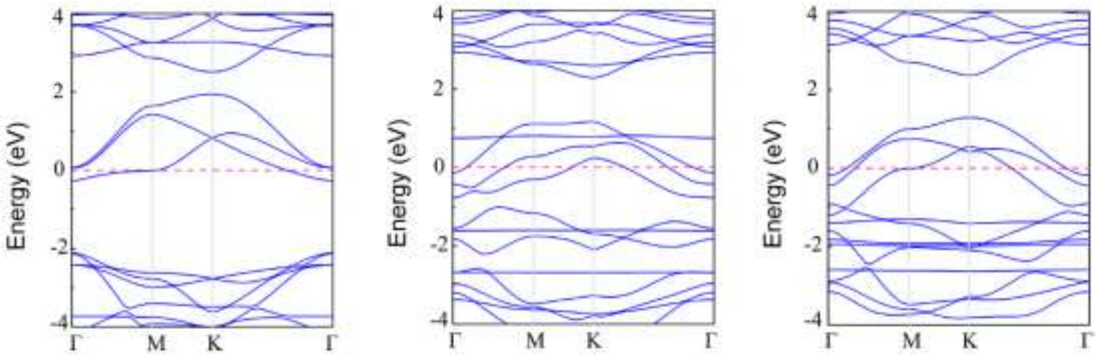

$Ag_1@C_2N$ $Ir_2@C_2N$ $Pt_2@C_2N$

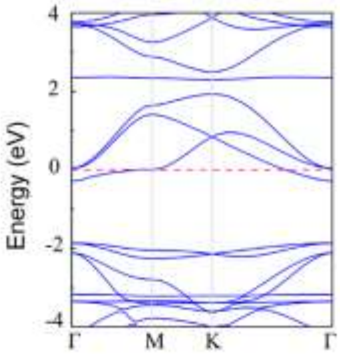

$Au_1@C_2N$

Fig. S3 Band structures of $TM_x@C_2N$ near Fermi level computed by HSE06. The Fermi level is set to zero. For $Ti_1@C_2N$, $Mn_1@C_2N$, $Fe_2@C_2N$, $Co_2@C_2N$ and $Ru_2@C_2N$, the origin represents spin-up and blue means spin-down.

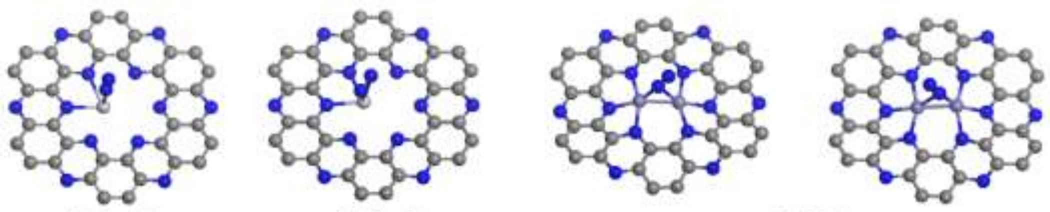

-0.62 eV -0.13 eV -0.59 eV

Ti_1@C_2N Fe_2@C_2N

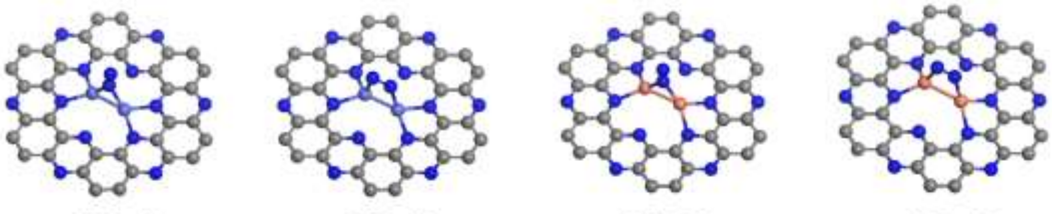

-0.80 eV -0.38 eV -0.47 eV -0.15 eV

Co_2@C_2N Cu_2@C_2N

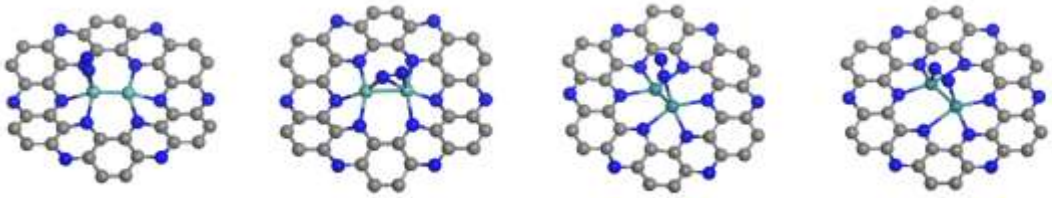

-0.08 eV -0.61 eV -0.28 eV 0.18 eV

Mo_2@C_2N Ru_2@C_2N

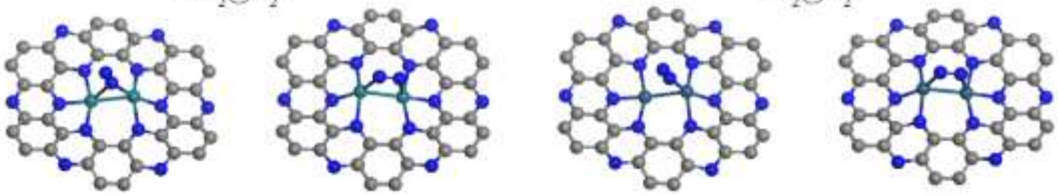

-0.72 eV -0.30 eV -0.96 eV -0.31 eV

Rh_2@C_2N Ir_2@C_2N

Fig. S4 Optimized structures and Gibbs free energy change of N_2 adsorption on TM_x@C_2N in standing-on and lying-on configurations.

In order to evaluate the reliability of the results computed in a unit cell, the adsorption energies of N_2 and N_2H on $Mo_2@C_2N$ in a 2×2×1 supercell were also calculated and are shown in Table S1. The difference of the computed adsorption energies is lower than 3%, indicating that the results computed in a unit cell is acceptable in this work.

Table S1. Adsorption energies (eV) of N_2 and N_2H on the $Mo_2@C_2N$ in a 2×2×1 supercell.

	1×1	2×2
N_2	-1.17	-1.20
N_2H	-3.53	-3.62

Table S2. Gibbs free energy change (eV) for the N_2 fixation of distal mechanisms on $TM_x@C_2N$.

	Ti_1	Co_2	Cu_2	Ru_2	Rh_2	Ir_2
$*N_2+H^++e^-\rightarrow *N\text{-}NH$	0.77	0.41	0.85	0.55	0.53	1.33
$*N\text{-}NH+H^++e^-\rightarrow *N\text{-}NH_2$	0.54	-0.11		0.31	0.59	-
$*N\text{-}NH_2+H^++e^-\rightarrow *N\text{-}NH_3$	-	-0.38		-0.27	-	-
$*N\text{-}NH_3\rightarrow *N+NH_3$	-	-0.22		-0.25	-	-
$*N+H^++e^-\rightarrow *NH$	-	-0.69		-0.36	-	-

Table S3. Energy barriers (eV) for the N_2 fixation of distal mechanisms on $TM_x@C_2N$.

	Ti_1	Co_2	Cu_2	Ru_2	Rh_2	Ir_2
$*N_2+H^++e^-\rightarrow *N\text{-}NH$	0.64	0.66	0.30	0.15	0.16	1.35
$*N\text{-}NH+H^++e^-\rightarrow *N\text{-}NH_2$	1.14	0.40	-	0.28	1.24	
$*N\text{-}NH_2+H^++e^-\rightarrow *N\text{-}NH_3$	-	-	-	0.04	-	
$*N+H^++e^-\rightarrow *NH$	-	0.83	-	0.81	-	

Table S4. Gibbs free-energy change (eV) for the N_2 fixation of alternating mechanisms on $TM_x@C_2N$.

	Ti_1	Rh_2
$*N_2+H^++e^-\rightarrow *N\text{-}NH$	0.77	0.53
$*N\text{-}NH+H^++e^-\rightarrow *NH\text{-}NH$	1.37	0.65

Table S5. Energy barriers (eV) for the N_2 fixation of alternating mechanisms on $TM_x@C_2N$.

	Ti_1	Rh_2
$*N_2+H^++e^-\rightarrow *N\text{-}NH$	0.64	0.16
$*N\text{-}NH+H^++e^-\rightarrow *NH\text{-}NH$	1.14	1.39

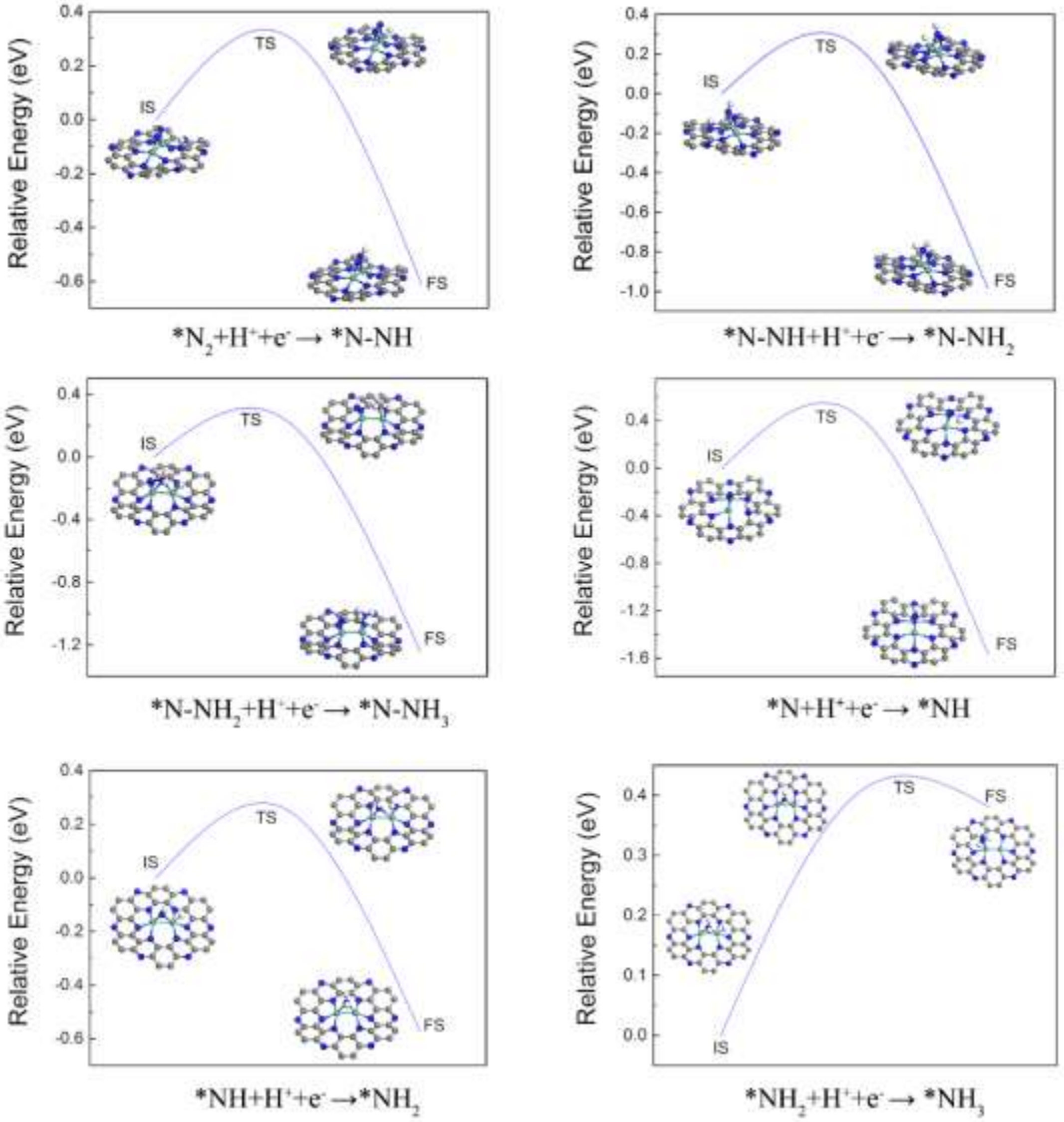

$*N_2+H^++e^-\rightarrow *N\text{-}NH$

$*N\text{-}NH+H^++e^-\rightarrow *N\text{-}NH_2$

$*N\text{-}NH_2+H^++e^-\rightarrow *N\text{-}NH_3$

$*N+H^++e^-\rightarrow *NH$

$*NH+H^++e^-\rightarrow *NH_2$

$*NH_2+H^++e^-\rightarrow *NH_3$

Fig. S5 Reaction pathway and energy barriers of N_2 fixation on $Mo_2@C_2N$ catalysts.

Table S6. Gibbs free-energy change (ΔG, eV), energy barriers ($E_{barrier}$, eV) and activation barriers ($E_{activation}$, eV) for the N_2 fixation on $Mo_2@C_2N$.

	ΔG	$E_{barrier}$	$E_{activation}$
$*+N_2\rightarrow*N_2$	-0.60	-	-
$*N_2+H^++e^-\rightarrow*N\text{-}NH$	0.33	0.31	-
$*N\text{-}NH+H^++e^-\rightarrow*N\text{-}NH_2$	-0.01	0.25	0.02
$*N\text{-}NH_2+H^++e^-\rightarrow*N\text{-}NH_3$	-1.00	0.31	0.66
$*N\text{-}NH_3\rightarrow*N+NH_3$	0.29	-	-
$*N+H^++e^-\rightarrow*NH$	-0.96	0.51	0.85
$*NH+H^++e^-\rightarrow*NH_2$	0.41	0.25	-
$*NH_2+H^++e^-\rightarrow*NH_3$	0.38	0.44	-
$*NH_3\rightarrow*+NH_3$	0.49	-	-

The activation barriers were calculated according to previous reports[1] based on:

$$E_{activation}(U)= E^0_{activation}\left(U^0\right)+ \beta'(U-U^0)$$

in which $E^0_{activation}$ is the barrier obtained from DFT with zero-point vibrational energy correction. U^0 is the equilibrium potential for the reductive adsorption of a proton. The chemical potential of adsorbed H is equal to that of a proton-electron pair. U is the electrode potential and -0.41 V is used here. β' is obtained:

$$\beta' = \beta + (\mu_{TS}-\mu_{reactant})/d$$

where β and d are 0.5 and 3, which are consistent with the previous report.[1]

References

1. X. Nie, M. R. Esopi, M. J. Janik and A. Asthagiri, Angew. Chem. Int. Ed., 2013, 52, 2459-2462.

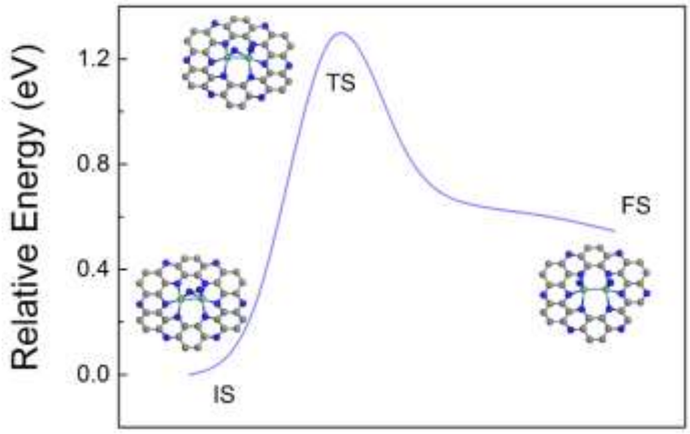

Fig. S6 Energy barrier for the direct dissociative process of N_2 on $Mo_2@C_2N$.

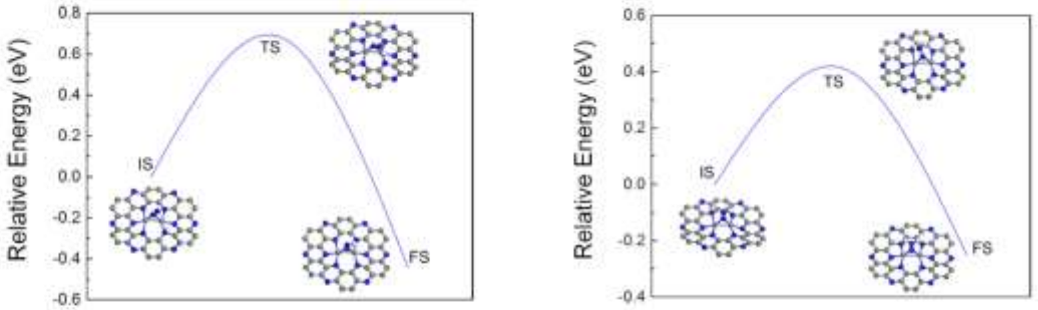

$*N_2+H^++e^- \rightarrow *N\text{-}NH$ $*N\text{-}NH+H^++e^- \rightarrow *N\text{-}NH_2$

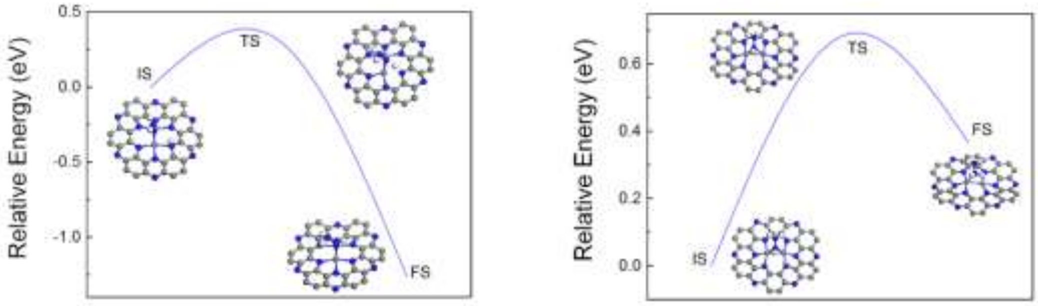

$*N\text{-}NH_2+H^++e^- \rightarrow *NH\text{-}NH_2$ $*NH\text{-}NH_2+H^++e^- \rightarrow *NH_2\text{-}NH_2$

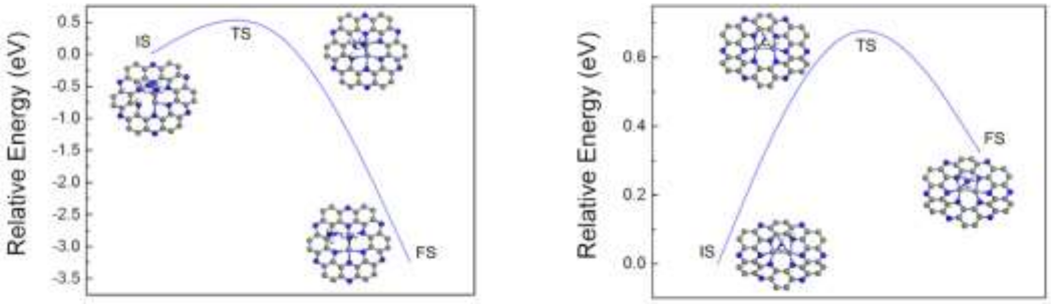

$*NH_2\text{-}NH_2+H^++e^- \rightarrow *NH_2\text{-}NH_3$ $*NH_2+H^++e^- \rightarrow *NH_3$

Fig. S7 Reaction pathway and energy barriers of N_2 fixation on $Fe_2@C_2N$ catalysts.